Thin film deposition with enhanced physiochemical properties using a novel RF atmospheric pressure plasma jet

Mehrnoush Narimisa[1], Yuliia Onyshchenko[1], Rino Morent[1], Nathalie De Geyter[1]

[1]*Research Unit Plasma Technology (RUPT), Department of Applied Physics, Faculty of Engineering and Architecture, Ghent University, Ghent, Belgium*

Abstract: A novel atmospheric pressure plasma jet set-up based on a three-gas layer geometry is introduced and the device potential for plasma-assisted polymerization of styrene was explored. The plasma effluent was characterized by Schlieren imaging while the coatings were analyzed using X-ray photoelectron spectroscopy (XPS) and atomic force microscopy (AFM). The outcomes indicate that the MPPJ3 configuration provides an effective gas mixing which results in a coating with enhanced properties analogue to polystyrene.

Keywords: APPJ, plasma polymerization, Schlieren imaging, polystyrene.

1. Introduction

Deposition of functional thin films is required in numerous applications such as packaging, electronics, tissue engineering, and aerospace industry. These thin films can be exploited as protection, barrier coatings, adhesion promotion, or preservation of special electrical, optical or mechanical properties [1]. Non-thermal plasma polymerization is one of the most suitable processes for thin film deposition due to its simplicity, one-step procedure, solvent-free aspect, and the non-invasive character which prevents any damage to the mechanical bulk properties of fragile materials [2]. A well-known dielectric barrier discharge (DBD) with parallel plates configuration is typically used for plasma polymerization purposes. However, a more flexible and promising atmospheric pressure plasma jet (APPJ) becomes more popular in use for this type of plasma processes [3].

In APPJ-assisted polymerization, there are two common methods for monomer injection into the plasma: 1) downstream of the plasma using an independent inlet or 2) upstream of the plasma together with the discharge gas [4-6]. In the former case, fragmentation of the monomer only occurs due to the interaction with the long-time living active species of the plasma. Moreover, the direction of the monomer injection can significantly influence the homogeneity of the coating [7]. Although it favors an enhanced polymerization process, the latter method causes monomer deposition onto the capillary walls which can reduce the lifetime of the device as well as influence its performance. Besides the direction of monomer injection, another challenge for plasma polymerization using APPJ methods is to preserve the monomer functional groups in the final coatings, as the monomer-plasma interactions mostly result in some sort of precursor fragmentation or incomplete polymerization. Therefore, obtaining a plasma-polymerized layer while preserving the monomer's original functionality is of significant importance in APPJ polymerization [8, 9]. As such, this work introduces a novel APPJ configuration, named MPPJ3, and focuses on examining the potential of the device for plasma polymerization of styrene as an important material with a wide range of applications such as humidity sensors, optical biosensors, protective coatings, biomedical application. In short, the device consists of three separated gas channels: (1) an inner channel which carries the plasma discharge gas, (2) a middle channel used to inject precursor and (3) an outer channel which acts as shielding gas beside providing a chemistry-rich environment for polymerization. A separated gas channel in this configuration, used for monomer introduction, helps to avoid deposition of the polymerized monomer on the inner walls of the capillary since the injection into the discharge only occurs at the outlet of the device. In addition, this device allows to introduce three different gases simultaneously into the system without mixing them in advance. In this work, particular attention is paid to analyzing the impact of the outer gas channel on the plasma polymerization behavior and to compare the outcomes with the inner + middle active channels while fixing all the other plasma deposition parameters. Indeed, when the inner and the middle channels are fed by argon and argon carrying precursor, respectively, polymerization is occurring in the plasma afterglow instead of in the active plasma region which is identical to the typical monomer injection from the downstream configuration, while the addition of the third gas layer has an exceptional influence on the overall plasma behavior and chemistry. As such, the effect of the outer gas layer on the physical and chemical properties of the MPPJ3 styrene-based coatings using the Schlieren imaging technique, AFM, and XPS will be examined.

2. Methods and materials

Fig. 1 illustrates the schematic representation of the experimental set-up whereas the experimental parameters are introduced in Table 1. The MPPJ3 set-up contains an inner quartz (internal diameter (ID)=1.3 mm) capillary. An RF powered tungsten rod with a diameter of 0.5 mm is centered inside the inner capillary. Coaxial to the inner capillary, another quartz tube (ID=4 mm) for introduction of monomer containing gas is located. Finally, a grounded outer hollow aluminum cylinder (ID=8 mm) has been arranged to act as an outer gas channel while maintaining the coaxial symmetry. Furthermore, an aluminum cap with a circular opening of 4.5 mm has been adjusted via a thread on the aluminum cylinder. The plasma jet set-up was powered with an RF generator CESAR 136, Advanced Energy, operating at 13.56 MHz using a matching box. Argon (Air Liquide, Alphagaz 1) was used as feed gas and monomer carrier gas. To deliver evaporated styrene

molecules into the system, argon was passed through a glass bubbler filled with styrene and the gas containing monomer was directed to the middle channel.

Two different plasma modes were generated depending on activating/inactivating the outer channel. If only the inner and middle channels are fed by argon and argon containing monomer, respectively, applying RF power to the tungsten wire leads to typical α-mode plasma ignition on the tip of the high voltage electrode (Fig. 1. b)). However, activating the outer channel by argon plasma contributes to the formation of a wider plasma plume which fills the volume inside the cap and thus the diameter of the plasma jet followed the nozzle outlet revealing the increased plasma size in this mode (Fig. *1*. c)). The outer channel further acts as shielding curtain limiting the atmospheric impact on plasma formation, and ensures the homogeneous mixing of the monomer containing middle gas stream with the plasma.

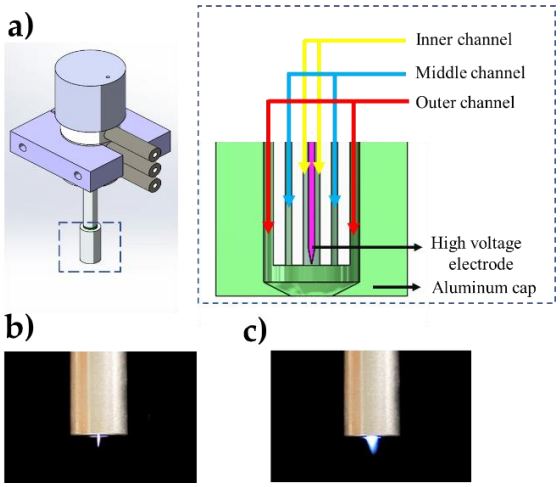

Fig. 1. a) Schematic representation of the MPPJ3 set-up together with the operational plasma b) without and c) with the third gas channel on.

Table 1. An overview of the applied experimental parameters (slm= standard liter per minute; sccm= standard cubic centimeter per minute).

Experimental conditions	
Input power	10 W
Plasma gas	Argon
Precursor	Styrene
Substrate	Glass, R_q = 6 ± 2 nm
Inner channel flow rate	0.5 slm
Middle channel flow rate	250 sccm
Outer channel flow rate	0 and 2 slm
Deposition time	5 min
Deposition speed	2 mm/s
Moving distance	30 mm

To observe the patterns of perturbation, typical Z-type Schlieren imaging was employed. Two parabolic mirrors (Edmund Optics) with f/10 aperture, 20.32 cm diameter, and 203.2 cm focal length were oriented at a 6° angle with respect to the horizontal axis and placed 310 cm apart. As a point light source, a warm white (3000 K) LED working in continuous mode was used. During the experiments, the plasma set-up was placed between the two mirrors in the parallel light beam. The camera (Nikon D3200) was focused on the plasma effluent, and photos were captured utilizing DigiCamControl software. A knife was mounted close to the camera lens to block the refocused light.

The thickness and the roughness of the deposited coatings were obtained by means of an XE-70 AFM apparatus (Park Scientific Instruments). For thickness measurements, a scratch was made with a sharp blade on the surface of the cover slip glass covered by the coating prior to the measurements. The non-contact tapping mode using a highly doped single crystal silicon cantilever with a spring constant of approximately 40 N/m was used to collect AFM images. The selected scan size was 18 × 18 μm^2. Subsequently, the data were analyzed using XEP software.

Finally, the chemical composition of the surface of the coated films was obtained by XPS. The measurements were carried out with a PHI Versaprobe II spectrometer. A monochromatic Al K_α X-ray source ($h\nu$ = 1486.6 eV) operating at 50 W was employed. The measurements were conducted in a vacuum of at least 10^{-6} Pa with a pass energy of 187.85 eV in steps of 0.8 eV at a take-off angle of 45° relative to the sample surface. High-resolution C1s peaks were also curve-fitted after calibration of the binding energy scale was performed using the hydrocarbon component of the C1s spectrum (285.0 eV). Afterwards, C1s peaks were curve-fitted utilizing Gaussian-Lorentzian peak shapes and the full width at half maximum (FWHM) of each inserted peak was constrained below 1.4 eV.

3. Results and discussions

Flow visualization through the Schlieren technique enables collecting useful information on the plasma propagation pattern and the laminarity length [10]. Therefore, Schlieren photos were taken with and without the outer gas channel on and the images are presented in Fig. 2. The results indicate that when only the inner and middle channels are in use (see Fig. 2 a)), the flow transits to the turbulent regime closer to the nozzle outlet. Interestingly, adding 2 slm of argon to the outer gas channel enhances the length of the laminar flow (Fig. 2 b)). Under this condition, additional mixing occurs inside the reusable cap. This extra volume provides time and space to form a “united” stream that flows out from the nozzle. This outcome predicts that using the three-gas channel configuration may result in a coating with less air admixture. In fact, in the turbulent regime, species from the ambient air such as oxygen can mix with the plasma

reactive species, absorb their energy, and further expand the plasma. In APPJ-assisted polymerization, these species can react with the dissociated monomer molecules in the plasma, generate other gas phase products, and subsequently, influence the resultant coating in terms of chemical composition.

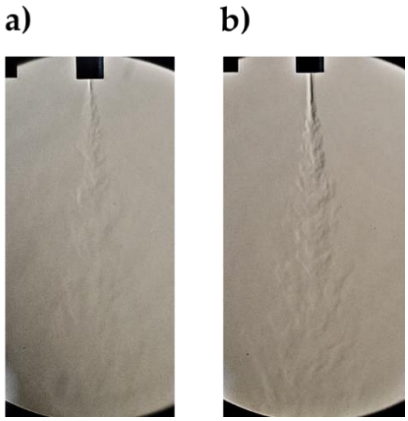

Fig. 2. Schlieren images of the MPPJ3 effluents while plasma was operational a) without and b) with the outer gas channel on.

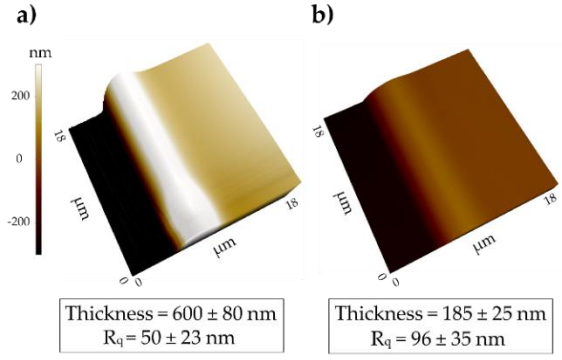

Fig. 3. AFM 3D representation of the scratched coated film on the glass substrate using MPPJ3 a) with and b) without the outer gas channel on.

The thickness and roughness of the coating are other important parameters indicating the physical quality of the coating and the plasma polymerization efficiency and the results are shown in Fig. 3. These results obtained from AFM imaging suggest that when using all three channels in the plasma jet, the obtained coating was almost three times thicker than the one obtained with only two working channels (inner and middle channel). Furthermore, the overall roughness of the latter sample was higher. This outcome suggests that under this particular experimental condition, an effective mixing between plasma and the precursor is not occurring. The reason behind this is when the plasma is formed through the inner channel and the precursor is fed to the system through the middle channel, not all monomer molecules are involved in the polymerization process and an incomplete polymerization might occur. On the other hand, with the active outer channel, the monomer molecules are trapped between the 2 gas streams and an effective mixing between the plasma effluent and the monomer containing channel occurs resulting in an adequate monomer dissociation and successive polymerization, as in this case more monomer molecules are involved in the polymerization process. It is worth mentioning that due to the enlarged plasma size in the three-gas layer configuration, the width of the coated layer (≈ 17 mm) was approximately two times bigger than the other counterpart (≈ 9 mm). Overall, the AFM results show that the efficiency of the coating formation is more pronounced in the presence of an outer gas layer.

Finally, XPS analysis was carried out to identify the surface chemical groups present on the plasma-polymerized styrene deposited on the glass substrates. Furthermore, through mapping over the substrate, XPS can provide valuable information on the chemical uniformity and the chemical distribution of the coating. To do so, measurements have been performed perpendicular to the jet movement direction and XPS survey scans were collected over a 2.5 mm radial distance for every 1 mm passing through the central treatment point (0 mm distance). The presence of the coating was confirmed by analyzing the Si signal, which is only present on the substrate since the deposited coating only contains C and O. **Error! Reference source not found.** Fig. 4 a) shows the XPS profile for the Si signal using the two experimental conditions. The figure illustrates that when only the inner and middle channels are in use (the black curve), the coating is deposited in a narrower region. Moreover, the pronounced shift of the curve towards the right-hand side of the graph also shows that the deposited coating is not homogeneously deposited across the line. However, when all three channels are simultaneously in use, the plasma-polymerized coating uniformly spreads across the deposited line, and the deposition area is also significantly wider in comparison to the two active channels set-up. Additional information regarding the surface functional groups can be obtained by curve fitting of the high-resolution C1s peaks of the coated samples. Fig. 4 b) and c) illustrate the deconvolution of the C1s peak obtained for both experimental conditions at a distance of 1.5 mm away from the center. The grey colored peaks positioned at 284.7, 285.0 and 291.3 eV represent the chemical fingerprint of polystyrene. One of the main challenges of atmospheric pressure plasma deposition is the presence of additional oxygen functionalities in the resulting coating. In fact, the presence of oxygen in the discharge due to gas impurities and ambient air admixing or post-treatment exposure of the sample induces oxygen functionalities in the deposited layers. As can be seen from this figure, when the outer layer of gas is not fed into the system, more oxygen-containing functionalities are present in the coating, whereas in the other case, the coating is less

oxidized. It means that using the outer channel also works as a “shielding gas” to minimize the plasma mixing with the surrounding atmosphere. The higher oxygen incorporation in the two-gas layer configuration was also evident in the Schlieren image where the transition to the turbulent flow occurred in the vicinity of the jet outlet. Finally, by analyzing the presence of the chemical groups on the surface of the coatings, it is possible to distinguish the peaks characteristics for polystyrene (as was done here). When only the inner and middle channels were used, only 19% of all detected carbon could be ascribed as originating from polystyrene, while this percentage was above 43% for the plasma-polymerized coating when all three gas channels were active.

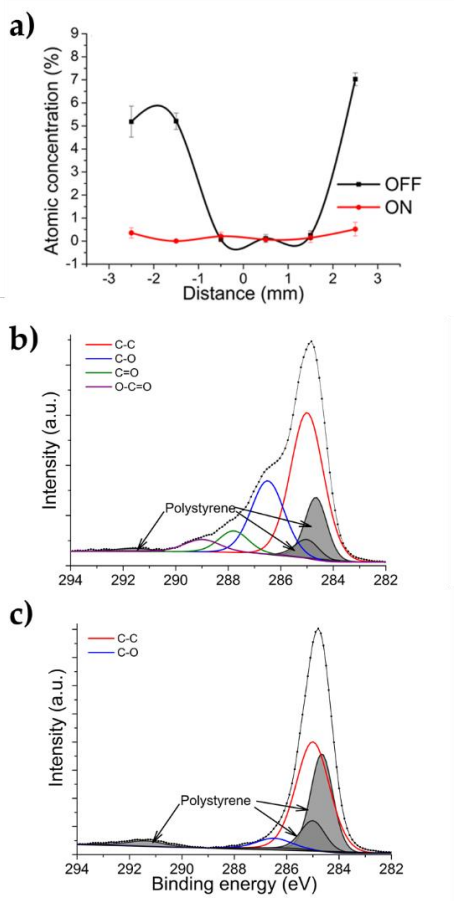

Fig. 4. a) XPS profile of the Si atomic concentration of plasma-polymerized styrene (OFF: outer gas channel not used, ON: outer gas channel used). C1s deconvoluted peaks for plasma-polymerized styrene deposited on glass substrates b) without and c) with the outer gas channel on.

4. Conclusion

In conclusion, this contribution presents a novel APPJ device for thin film fabrication using a three-gas curtain configuration. With the success in the design of the plasma jet device, a high deposition efficiency and a decent mixing of gas layers in the plasma active region were reached. The XPS and AFM findings showed that by adding the third gas layer, the plasma-polymerized film revealed an enhanced chemical and physical uniformity. The XPS results further illustrated that, by using all three gas layers, low oxidation of the coating and high spectral resemblance to classically polymerized polystyrene was obtained, which suggested that the third gas layer had both shielding and mixing effects.

5. References

[1] P. M. Martin, *Handbook of deposition technologies for films and coatings: science, applications and technology*. William Andrew, 2009.

[2] D. Merche, N. Vandencasteele, and F. Reniers, "Atmospheric plasmas for thin film deposition: A critical review," *Thin Solid Films*, vol. 520, no. 13, pp. 4219-4236, 2012.

[3] F. Fanelli and F. Fracassi, "Atmospheric pressure non-equilibrium plasma jet technology: general features, specificities and applications in surface processing of materials," *Surface and Coatings Technology*, vol. 322, pp. 174-201, 2017.

[4] J. Pulpytel, V. Kumar, P. Peng, V. Micheli, N. Laidani, and F. Arefi-Khonsari, "Deposition of Organosilicon Coatings by a Non-Equilibrium Atmospheric Pressure Plasma Jet: Design, Analysis and Macroscopic Scaling Law of the Process," *Plasma Processes and Polymers*, vol. 8, no. 7, pp. 664-675, 2011.

[5] M. D. Barankin, T. S. Williams, E. Gonzalez II, and R. F. Hicks, "Properties of fluorinated silica glass deposited at low temperature by atmospheric plasma-enhanced chemical vapor deposition," *Thin Solid Films*, vol. 519, no. 4, pp. 1307-1313, 2010.

[6] Y. Ito, O. Sakai, and K. Tachibana, "Study of plasma enhanced chemical vapor deposition of ZnO films by non-thermal plasma jet at atmospheric pressure," *Thin Solid Films*, vol. 518, no. 13, pp. 3513-3516, 2010.

[7] M. Narimisa, F. Krčma, Y. Onyshchenko, Z. Kozáková, R. Morent, and N. De Geyter, "Atmospheric pressure microwave plasma jet for organic thin film deposition," *Polymers*, vol. 12, no. 2, p. 354, 2020.

[8] P. Dubruel and S. Vlierberghe, "Biomaterials for bone regeneration: novel techniques and applications," 2014.

[9] M. Bashir and S. Bashir, "Hydrophobic–hydrophilic character of hexamethyldisiloxane films polymerized by atmospheric pressure plasma jet," *Plasma Chemistry and Plasma Processing*, vol. 35, no. 4, pp. 739-755, 2015.

[10] E. Traldi *et al.*, "Schlieren imaging: a powerful tool for atmospheric plasma diagnostic," *EPJ*

Techniques and Instrumentation, vol. 5, pp. 1-23, 2018.